Brazilian Journal of Medical and Biological Research Online Provisional Version
ISSN 0100-879X

Lymphatic fluctuation in the parenchymal remodeling stage of acute interstitial pneumonia, organizing pneumonia, nonspecific interstitial pneumonia and idiopathic pulmonary fibrosis

E.R. Parra, C.A.L. Araujo, J.G. Lombardi, A.M. Ab'Saber, C.R.R. Carvalho, R.A. Kairalla and V.L. Capelozzi

Departamento de Patologia, Faculdade de Medicina, Universidade de São Paulo, São Paulo, SP, Brasil

Abstract

Because the superficial lymphatics in the lungs are distributed in the subpleural, interlobular and peribroncovascular interstitium, lymphatic impairment may occur in the lungs of patients with idiopathic interstitial pneumonias (IIPs) and increase their severity. We investigated the distribution of lymphatics in different remodeling stages of IIPs by immunohistochemistry using the D2-40 antibody. Pulmonary tissue was obtained from 69 patients with acute interstitial pneumonia/diffuse alveolar damage (AIP/DAD, N = 24), cryptogenic organizing pneumonia/organizing pneumonia (COP/OP, N = 6), nonspecific interstitial pneumonia (NSIP/NSIP, N = 20), and idiopathic pulmonary fibrosis/usual interstitial pneumonia (IPF/UIP, N = 19). D2-40+ lymphatic in the lesions was quantitatively determined and associated with remodeling stage score. We observed an increase in the D2-40+ percent from DAD (6.66 ± 1.11) to UIP (23.45 ± 5.24, P = 0.008) with the advanced process of remodeling stage of the lesions. Kaplan-Meier survival curves showed a better survival for patients with higher lymphatic D2-40+ expression than 9.3%. Lymphatic impairment occurs in the lungs of IIPs and its severity increases according to remodeling stage. The results suggest that disruption of the superficial lymphatics may impair alveolar clearance, delay organ repair and cause severe disease progress mainly in patients with AIP/DAD. Therefore, lymphatic distribution may serve as a surrogate marker for the identification of patients at greatest risk for death due to IIPs.

Key words: Lymphangiogenesis; Lymphatic vessel; Idiopathic interstitial pneumonias; Lung remodeling; Immunohistochemistry; Morphometry

Introduction

Pulmonary fluid homeostasis is modulated by the balance between fluid filtration into the pulmonary interstitium from blood capillaries and its removal from the interstitium via the lymphatic system (1-5). Impairment of pulmonary lymphatic flow due to several pathological situations such as pulmonary edema results in excess fluid accumulation within the pulmonary interstitium, which often leads to interstitial fibrosis, pleural effusion and subsequent pulmonary dysfunction (1,2). In the mammalian lung, lymph is drained from the subpleural lymphatic plexus to the periaxial lymphatic plexus through interlobular lymphatic channels (6). These pulmonary lymphatic networks have been repeatedly investigated in detail in humans and animals by observations using dye-injection techniques, electron microscopy and lymphangiography (5). However, these techniques are inappropriate for histopathological observation of the lymphatic system in formalin-fixed paraffin-embedded tissues obtained from lung tissues.

Correspondence: V.L. Capelozzi or E.R. Parra, Departamento de Patologia, Faculdade de Medicina, USP, Av. Dr. Arnaldo, 455, 01246-903 São Paulo, SP, Brasil. Fax: +55-11-3064-2744. E-mail: vcapelozzi@lim05.fm.usp.br or erparra20003@yahoo.com.br

Received November 7, 2011. Accepted March 21, 2012. Available online April 13, 2012.

In idiopathic interstitial pneumonias (IIPs), parenchymal remodeling after alveolar damage results in scar formation through several sequential stages of epithelial cell necrosis, alveolar collapse, apposition of alveolar septa, and fibrosis (7). In the process of pulmonary remodeling, the viable epithelial cells around the lesion express cytoprotective proteins and cytokines, which facilitate the remodeling of the affected lesion (8). Pulmonary remodeling is, thus, dependent on various contributors, and vascular factors are critical for angiogenesis in the healing area (9,10). Vascular factors are promptly expressed in the surviving alveolar epithelium around the infarcted lesion after injury (11,12). The process of angiogenesis and lymphagiogenesis in the remodeling process of IIPs has been investigated sporadically (9-14). This is probably due to the lack of a reliable marker that can distinguish the lymphatic endothelium from the blood capillary endothelium. In recent years, lymphatic endothelial cell-specific proteins have been identified, including VEGF receptor-3, lymphatic endothelial hyaluronan receptor-1 (LYVE-1), podoplanin, prox-1, D6 and D2-40 (15,16). In the lung, recent studies have reported lymphatic morphology and density in diffuse alveolar damage (DAD) and organizing pneumonia (OP) by immunohistochemistry but did not include nonspecific interstitial pneumonia (NSIP) or usual interstitial pneumonia (UIP) (13,14). Because the superficial lymphatics in the lungs are distributed in the subpleural, interlobular and peribroncovascular interstitium, we hypothesized that lymphatic impairment would occur in the lungs of IIPs and increase their severity. In the present study, we investigated lymphatic distribution in the entire process of parenchymal remodeling in DAD, OP, NSIP, and UIP by immunohistochemistry using the D2-40 antibody which, is considered to be the most sensitive and specific marker for lymph vessel endothelium (16). Furthermore, the impact of these findings was evaluated as a function of physiological testing and survival of the patients.

Patients and Methods

Patient selection

Pulmonary tissue was obtained from 69 surgical lung biopsies from patients with IIPs. The biopsies were classified according to the American Thoracic Society/European Respiratory Society (ATS/ERS) consensus classification (17). A remodeling stage score was attributed to each group and included:

Diffuse alveolar damage. DAD was characterized by involvement and a uniform temporal appearance caused by alveolar collapse, hyaline membrane, septal inflammation, and obliterative organizing fibrosis (17) (score 1), N = 24 cases (Figure 1A).

Organizing pneumonia. OP was characterized by a focal injury in the epithelial cell-epithelium basement membrane unit resulting in the formation of granulation tissue in the airspace consisting of single stalk, plump myofibroblasts embedded in an edematous stroma with mononucleated inflammatory cells, capillary vessels and moderate organizing fibrosis (17) (score 2), N = 6 cases (Figure 1C).

Nonspecific interstitial pneumonia cellular pattern. NSIP was characterized by temporally homogenous septal inflammatory thickening and minimal organizing fibrosis (17) (score 3), N = 20 cases (Figure 1E).

Usual interstitial pneumonia. UIP was defined by alternating areas of normal parenchyma, alveolar collapse, honeycombing, and severe mural organizing fibrosis, defined as sites of active remodeling overlying fibrous airspace walls, and thus showing temporal heterogeneity, or overlying normal rigid pulmonary structures (e.g., interlobular septa) in the form of fibroblast foci and granulation tissue (17) (score 4), N = 19 cases (Figure 1G).

All patients included exhibited clinical, radiological and physiological changes consistent with acute interstitial pneumonia (AIP), cryptogenic organizing pneumonia (COP), NSIP, or idiopathic pulmonary fibrosis (IPF). Two or three biopsy specimens per patient were sampled and the tissue were collected according to the high-resolution computed tomography pattern, which usually includes normal, intermediate and more affected areas in different parts of the lung. Thus, the diagnosis of our patients with IIPs was obtained by clinical, radiological and histological consensus criteria.

For semi-quantitative analysis, UIP histological pattern was divided into three different stages (10): alveolar collapse, mural organizing fibrosis and honeycomb. The UIP alveolar collapse stage was characterized by focal mural fibrosis, minimal inflammatory activity and sparse honeycombing transformation. In the UIP mural fibrosis stage, the pulmonary parenchyma showed a high degree of inflammatory activity, focal mural fibrosis and moderate parenchymal honeycombing changes. Pulmonary parenchyma showing extensive areas of mural fibrosis, fibroblastic foci and honeycomb remodeling corresponded to the third UIP stage (honeycombing). These three stages were evaluated by two experienced pathologists in the area.

Baseline characteristics

The median age of the patients was 47 years (range 19-74) for AIP (13 men, 10 women), 54 years (range 40-60) for COP (4 men, 2 women), 50.8 years (range 39-76) for NSIP (11 men, 9 women), and 66 years (range 48-76) for IPF (12 men, 7 women).

Physiological testing

The pulmonary function tests included forced expiratory volume in 1 s (FEV1), forced vital capacity (FVC), FEV1/FVC ratio 6100, total lung capacity (TLC), residual volume and carbon monoxide transfer factor (*D*LCO). TLC, residual volume and residual volume/TLC percentages were measured by the helium-dilution method with a Master Screen Apparatus (Erich Jaeger GmbH, Germany), and *D*LCO and *D*LCO/alveolar volume by the single breath-holding helium-dilution method (18). Lung function measurements are reported as percentages of predicted values. In all patients, arterial PaO_2 and $PaCO_2$ were also measured at rest. The cardiac parameters of these patients were normal.

Tissue preparation and immunohistochemistry

All pulmonary tissue was fixed in 10% neutral buffered formalin and embedded in paraffin. Thin sections were stained with hematoxylin and eosin. Additional subserial sections from all the paraffin blocks were used for immunohistochemistry. The antibody used was D2-40 (Signet Laboratory Inc., USA). Immunohistochemistry was performed using the Envision (+) kit (Dako Cytomation, USA) according to manufacturer instructions. Sections were visualized by treating the slides with diamino-benzidine-tetrahydrochloride. To demonstrate antibody specificity, sections from each paraffin block were used as negative controls by omitting the primary antibody and replacing it with normal mouse or rabbit immunoglobulin. Positive expression of D2-40 was indicated by brown cytoplasmic staining.

Morphometry

The sections immunostained with D2-40 antibody were observed by light microscopy at 400X magnification. Only vessels with a lumen or consisting of more than a single endothelial cell positive for D2-40 were considered to be lymphatic vessels. We used an eyepiece grid with 100 points and 50 lines to quantify the area and the lymphatics immunostained for D2-40+ as follows: Ten fields were chosen from across multiple sites accounting/adjusting for cellularity or as number of positively stained cells per mesenchymal tissue (19). In other words, the parenchymal area in each field was determined according to the number of points hitting on positive cells, as a proportion of the total grid area. Afterward, the number of positive cells within the parenchymal area was counted. The immunostaining cellularity was determined as the number of positive cells in each field divided by the parenchymal area. The final results are reported as means ± standard deviation (SD) of the lung specimens of each patient in 10 random, non-coincident microscopic fields.

To control for variation in scoring between our two histologists (ERP and VLC), 20% of the stained slides were independently scored by both observers. The coefficient of variance between cell counts for the two observers was <5%.

Statistical analysis

Data are reported as means ± SD. Statistical analysis was performed by analysis of variance followed by appropriate *post hoc* tests including the Student *t*-test for variables. Survival curves were determined by the Kaplan-Meier method and the risk of death was estimated by Cox regression. The statistical program used was SPSS, Inc. (USA). A P value less than 0.05 was considered to be significant.

Results

Distribution of lymphatic vessels according to pulmonary parenchymal remodeling stage score

In DAD, a few D2-40+ lymphatic vessels were identified in the region of thickened alveolar septa or in the peripheral interstitium of the affected area (Figure 1A and B).

In OP, we observed few D2-40 lymphatic vessels around the bronchovascular interstitium and in granulation tissue of the intraluminal plugs. The lymphatic vessels were tortuous and with minimal dilatation (Figure 1C and D).

In the NSIP pattern, we detected a few D2-40+ lymphatic vessels in the region of thickened alveolar septa. Lymphatic vessels were observed with more dilatation than in OP (Figure 1E and F).

In the UIP histological pattern, lymphatic vessels presented a large luminal area and were observed in the peripheral region and around fibroblastic foci (Figure 1G and H). Lymphatic vessels were increased in the interlobular and subpleural space.

Lymphatic distribution was significantly related to parenchymal remodeling score in DAD, OP, NSIP, and UIP. In other words, the organizing fibrosis present as obliterative (score 1) in DAD, the intraluminal plugs (score 2) observed in OP, the septal inflammatory thickening and minimal organizing fibrosis (score 3) of NSIP, and the mural organizing fibrosis and fibroblast foci (score 4) found in UIP were significantly related to the density of lymphatic vessels (Figure 2).

Fluctuation of lymphatic vessels according to pulmonary parenchymal remodeling stage score

Lymphatic D2-40+ in the four categorized lesions is indicated in Figure 2. Lymphatic D2-40+ differed significantly in the lesions of the four categories. D2-40 expression increased with the progression from DAD (6.66 ± 1.11), OP (15.35 ± 3.75), NSIP (15.49 ± 1.80), up to UIP (23.45 ± 5.24).

Pulmonary function tests and survival

Thirty-five patients died during the 180-month follow-up period (20 AIP, 1 COP, 5 NSIP, and 9 IPF). All patients studied had a restrictive lung function pattern characterized by a decrease in TLC (mean values were 57% of predicted values for AIP, 55% for NSIP and 75% for IPF) and an increase in FVC/FEV1 ratio (mean values were 97% of predicted values for AIP, 88% for COP, 109% for NSIP, and 118% for IPF). The mean predicted values of *D*LCO were decreased in patients with NSIP (51%) and IPF (53%). The pulmonary function of patients with AIP, COP, NSIP, and IPF and with different degrees of organizing fibrosis and lymphatic density did not differ significantly between groups. We analyzed the survival curves by comparing patient characteristics (baseline data and physiological test) and distribution and fluctuation of lymphatic vessels according to pulmonary parenchymal remodeling stage. Kaplan-Meier survival curves showed that patients with a 9.3% median lymphatic vessel density in lung parenchyma presented higher survival than patients with a <9.3% median lymphatic vessel density in lung parenchyma (125 *vs* 45 months, respectively). Multivariate analyses by the Cox regression model showed statistical significance (log likelihood = 61.98; P = 0.000) for low risk of death for patients <55 years (OR = 0.17) with OP (OR = 0.01) and with high FVC (OR = 0.9), whereas a high risk of death was found for male patients (OR = 6.73) and with lymphatic density <9.3% (OR = 11.03). Regression plots of survival probability versus follow-up time in months in patients with IIPs showed that the group with lymphatic density >9.3% had better survival than the group with <9.3% (Figure 3).

Discussion

The present study using morphometry revealed a large increase of the lymphatics in the interlobular and subpleural space, in which massive fibrosis increased with the development of new lymphatics in the lungs of patients with UIP. In contrast, in the lungs of patients with DAD, OP and cellular NSIP, a few lymphatics had extended into the alveolar lesions from the superficial lymphatics, especially into granulation tissues within the alveolar space. Although massive fibrotic diseases developed in IPF, including fibroblastic foci, lymphatic vessel density was increased in the lungs of UIP, probably draining excessive proteins and fluid. These results suggest that the increase of superficial lymphatics may improve alveolar clearance, accelerate organ repair and avoid disease progress in patients with IPF.

Lymphatic dilatation was not detected in the early stages of the remodeling process, but a few dilated lymphatics first appeared in the peripheral region adjacent to viable epithelial cells in the early process of fibroblastic foci. Lymphatic dilatation subsequently increased during the mural fibrosis period and was maintained thereafter during scar formation. In addition, LDE increased in the early stage of intraluminal granulation of OP and septal inflammatory thickening of NSIP, abruptly decreased in stages with DAD, but with a subsequent increase with the process of mural fibrosis in UIP. From these results, it can be seen that, during the entire process of parenchymal remodeling, the lymphatics mainly participate in fibrosis maturation and scar formation through the drainage of excessive proteins and fluid.

In the lung tissue of IIPs investigated in the present study, D2-40+ lymphatics were abundant in the subpleural regions, as well as in the interlobular interstitium. These findings are consistent with the distribution patterns of pulmonary lymphatics confirmed by other methods (5). In the light of lymphatic distribution, the abundant lymphatics in the subpleural region detected by D2-40 immunohistochemistry seem to correspond to the subpleural lymphatic plexus (6). Previous studies describing lymphatic distribution in sections of normal renal tissue (16,20) and other reports have also demonstrated the usefulness of D2-40 immunohistochemistry for detecting lymphatic capillaries in the renal interstitium (21).

Parenchymal remodeling after pulmonary injury is characterized by an increase in pulmonary endothelial and epithelial permeability. This early phase is followed by a subacute fibroproliferative phase that may allow repair of the injured lung or result in progressive obliteration of the interstitial and alveolar compartments of the lung by a fibroproliferative process that may be in fact established by 24 h after the injury (22). In this process of epithelial necrosis, extracellular matrices are degraded by inflammatory cell proteases (23-25). Based on such early events after the onset of parenchymal remodeling, it is supposed that pre-existing vascular tissues in the affected area also disintegrate through the influence of ischemia and inflammatory cells. The present results have clearly demonstrated that D2-40+ lymphatic vessels were poorly detected in the affected areas of early remodeling such as DAD, OP and NSIP compared to the UIP late stage. Lymphatics in the peripheral pulmonary interstitium consist of single-layered, thin endothelial cells, which possess an undeveloped basement membrane with no pericytes around them (6). These characteristics of lymphatic structures may cause vulnerability to ischemic damage and/or degradation by proteases, as is the case for blood capillaries.

In the present study, LDE surprisingly increased in the late mural fibrosis stage of UIP, when newly formed blood capillaries were usually decreased, as previously described by Parra et al. (10). In general, lymphangiogenesis develops through budding, sprouting and/or remodeling from pre-existing vessels, which frequently occur in pathological conditions, such as malignant tumors (26,27). In the process of cutaneous wound healing in the mouse model, lymphatics appear in subcutaneous tissue along the wound edge at 3-5 days after injury (28). It is therefore hypothesized that newly formed lymphatics first appear in the peripheral area of the lesion through sprouting from the pre-existing lymphatics around the lesion, and the proliferation of lymphatics follows after blood vessel angiogenesis.

In the current study, LDE significantly increased with healing maturation from the NSIP stage up to the UIP stage. These results indicate that lymphatics mainly participate in the maturation of fibrosis and/or scar formation through the drainage of excessive proteins and fluid. Based on these descriptions, including our results, it is considered that the role of lymphatics during parenchymal remodeling may be maintained for a longer time than that of blood vessels and that immunohistochemistry using a lymphatic endothelial marker is useful in investigating the role of lymphatics in IIPs.

Our study has clinical implications. In order to establish the relevance of these findings to patient evolution, lymphatic distribution in AIP/DAD, COP/OP, NSIP/NSIP, and IPF/UIP was evaluated in terms of physiological testing and survival. Clearly, multivariate analyses showed a low risk of death for female patients with OP and high FVC, but a high risk for males with median age >55 years and low lymphatic D2-40+ expression.

Finally, lymphatic distribution may serve as a surrogate marker for the identification of patients at greatest risk for death in IIPS.

Acknowledgments

Research supported by CNPq, FAPESP (#07/52785-0, #08/53022-3 and #08/57130-5), Laboratório Diagnóstika, Hospital das Clínicas and Faculdade de Medicina, Universidade de São Paulo.

References

1. Aharinejad S, Bock P, Firbas W, Schraufnagel DE. Pulmonary lymphatics and their spatial relationship to venous sphincters. *Anat Rec* 1995; 242: 531-544.
2. Bernaudin JF, Fleury-Feith J. [Structure and physiology of the pleura and the pleural space]. *Rev Pneumol Clin* 2006; 62: 73-77.
3. Shinohara H. Distribution of lymphatic stomata on the pleural surface of the thoracic cavity and the surface topography of the pleural mesothelium in the golden hamster. *Anat Rec* 1997; 249: 16-23.
4. Azzali G. The lymphatic vessels and the so-called “lymphatic stomata” of the diaphragm: a morphologic ultrastructural and three-dimensional study. *Microvasc Res* 1999; 57: 30-43.
5. Marchetti C, Poggi P, Clement MG, Aguggini G, Piacentini C, Icaro-Cornaglia A. Lymphatic capillaries of the pig lung: TEM and SEM observations. *Anat Rec* 1994; 238: 368-373.
6. Ohtani O, Ohtani Y. Organization and developmental aspects of lymphatic vessels. *Arch Histol Cytol* 2008; 71: 1-22.
7. White ES, Lazar MH, Thannickal VJ. Pathogenetic mechanisms in usual interstitial pneumonia/idiopathic pulmonary fibrosis. *J Pathol* 2003; 201: 343-354.
8. Selman M, King TE, Pardo A. Idiopathic pulmonary fibrosis: prevailing and evolving hypotheses about its pathogenesis and implications for therapy. *Ann Intern Med* 2001; 134: 136-151.
9. Parra ER, Kairalla RA, de Carvalho CR, Capelozzi VL. Abnormal deposition of collagen/elastic vascular fibres and prognostic significance in idiopathic interstitial pneumonias. *Thorax* 2007; 62: 428-437.
10. Parra ER, David YR, da Costa LR, Ab’Saber A, Sousa R, Kairalla RA, et al. Heterogeneous remodeling of lung vessels in idiopathic pulmonary fibrosis. *Lung* 2005; 183: 291-300.
11. Parra ER, Silverio da Costa LR, Ab’Saber A, Ribeiro de Carvalho CR, Kairalla RA, Fernezlian SM, et al. Nonhomogeneous density of CD34 and VCAM-1 alveolar capillaries in major types of idiopathic interstitial pneumonia. *Lung* 2005; 183: 363-373.
12. Ebina M, Shimizukawa M, Shibata N, Kimura Y, Suzuki T, Endo M, et al. Heterogeneous increase in CD34-positive alveolar capillaries in idiopathic pulmonary fibrosis. *Am J Respir Crit Care Med* 2004; 169: 1203-1208.
13. Yamashita M, Iwama N, Date F, Chiba R, Ebina M, Miki H, et al. Characterization of lymphangiogenesis in various stages of idiopathic diffuse alveolar damage. *Hum Pathol* 2009; 40: 542-551.
14. Mandal RV, Mark EJ, Kradin RL. Organizing pneumonia and pulmonary lymphatic architecture in diffuse alveolar damage. *Hum Pathol* 2008; 39: 1234-1238.
15. Akishima Y, Ito K, Zhang L, Ishikawa Y, Orikasa H, Kiguchi H, et al. Immunohistochemical detection of human small lymphatic vessels under normal and pathological conditions using the LYVE-1 antibody. *Virchows Arch* 2004; 444: 153-157.
16. Kahn HJ, Bailey D, Marks A. Monoclonal antibody D2-40, a new marker of lymphatic endothelium, reacts with Kaposi’s sarcoma and a subset of angiosarcomas. *Mod Pathol* 2002; 15: 434-440.
17. American Thoracic Society/European Respiratory Society. American Thoracic Society/European Respiratory Society International

Multidisciplinary Consensus Classification of the Idiopathic Interstitial Pneumonias. *Am J Respir Crit Care Med* 2002; 165: 277-304.
18. Quanjer PH, Tammeling GJ, Cotes JE, Pedersen OF, Peslin R, Yernault JC. Lung volumes and forced ventilatory flows. Report Working Party Standardization of Lung Function Tests, European Community for Steel and Coal. Official Statement of the European Respiratory Society. *Eur Respir J Suppl* 1993; 16: 5-40.
19. Gundersen HJ, Bendtsen TF, Korbo L, Marcussen N, Moller A, Nielsen K, et al. Some new, simple and efficient stereological methods and their use in pathological research and diagnosis. *APMIS* 1988; 96: 379-394.
20. Fukunaga M. Expression of D2-40 in lymphatic endothelium of normal tissues and in vascular tumours. *Histopathology* 2005; 46: 396-402.
21. Ishikawa Y, Akasaka Y, Kiguchi H, Akishima-Fukasawa Y, Hasegawa T, Ito K, et al. The human renal lymphatics under normal and pathological conditions. *Histopathology* 2006; 49: 265-273.
22. Rocco PR, Negri EM, Kurtz PM, Vasconcellos FP, Silva GH, Capelozzi VL, et al. Lung tissue mechanics and extracellular matrix remodeling in acute lung injury. *Am J Respir Crit Care Med* 2001; 164: 1067-1071.
23. Santos FB, Nagato LK, Boechem NM, Negri EM, Guimarães A, Capelozzi VL, et al. Time course of lung parenchyma remodeling in pulmonary and extrapulmonary acute lung injury. *J Appl Physiol* 2006; 100: 98-106.
24. Rocco PR, Facchinetti LD, Ferreira HC, Negri EM, Capelozzi VL, Faffe DS, et al. Time course of respiratory mechanics and pulmonary structural remodelling in acute lung injury. *Respir Physiol Neurobiol* 2004; 143: 49-61.
25. Negri EM, Hoelz C, Barbas CS, Montes GS, Saldiva PH, Capelozzi VL. Acute remodeling of parenchyma in pulmonary and extrapulmonary ARDS. An autopsy study of collagen-elastic system fibers. *Pathol Res Pract* 2002; 198: 355-361.
26. Ji RC. Lymphatic endothelial cells, lymphangiogenesis, and extracellular matrix. *Lymphat Res Biol* 2006; 4: 83-100.
27. Scavelli C, Weber E, Agliano M, Cirulli T, Nico B, Vacca A, et al. Lymphatics at the crossroads of angiogenesis and lymphangiogenesis. *J Anat* 2004; 204: 433-449.
28. Ji RC, Miura M, Qu P, Kato S. Expression of VEGFR-3 and 5'-nase in regenerating lymphatic vessels of the cutaneous wound healing. *Microsc Res Tech* 2004; 64: 279-286.

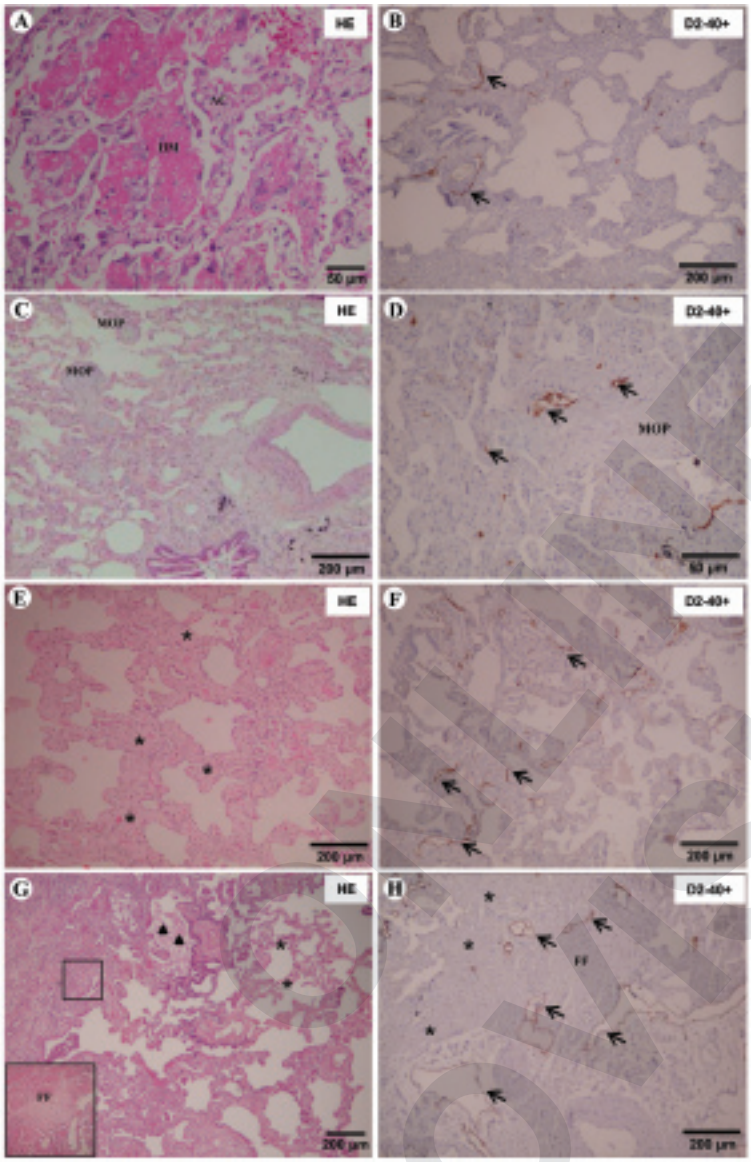

Figure 1. Histology of the diffuse alveolar damage (*A*,*B*), organizing pneumonia (*C*,*D*), nonspecific interstitial pneumonia (*E*,*F*), and usual interstitial pneumonia (*G*,*H*). Diffuse alveolar damage characterized by hyaline membranes (HM), alveolar collapse (AC), septal inflammation, and obliterative organizing fibrosis (*A*); note a few D2-40+ lymphatic vessels in the thickened alveolar region (arrows; *B*). Organizing pneumonia (*C*) showing prominent areas of myxoid organizing pneumonia (MOP) characterized by proliferation of plump fibroblasts embedded in an edematous stroma, forming intraluminal plugs in alveolar ducts and alveoli; anti-D2-40 immunohistochemical (*D*) stain decorates lymphatic lumens in organizing pneumonia; note peribronchial and intra-plug (MOP) (arrows) distribution of D2-40+. Nonspecific interstitial pneumonia (*E*) showing homogenous thickening of the alveolar septa by inflammatory cell proliferation (asterisks); anti-D240 immunohistochemical stain decorates lymphatic lumens in nonspecific interstitial pneumonia (arrows; *F*) in the peribronchovascular region, while the lumens are absent along the alveolar septa of the affected area. Usual interstitial pneumonia (*G*) showing alternating areas of normal parenchyma (asterisks), honeycombing (triangles) and organizing fibrosis with fibroblastic foci (FF), in detail; anti-D2-40 immunohistochemical stains lymphatics (arrows; *H*) with a large area or dilated in the peripheral region of honeycombing changes; note fibroblastic foci (FF) overlying the surface of the airspace or enlarged and remodeled airspaces with dense scars in the walls (asterisks). Hematoxylin and eosin (*A*-*D*). Peroxidase (*E*-*H*).

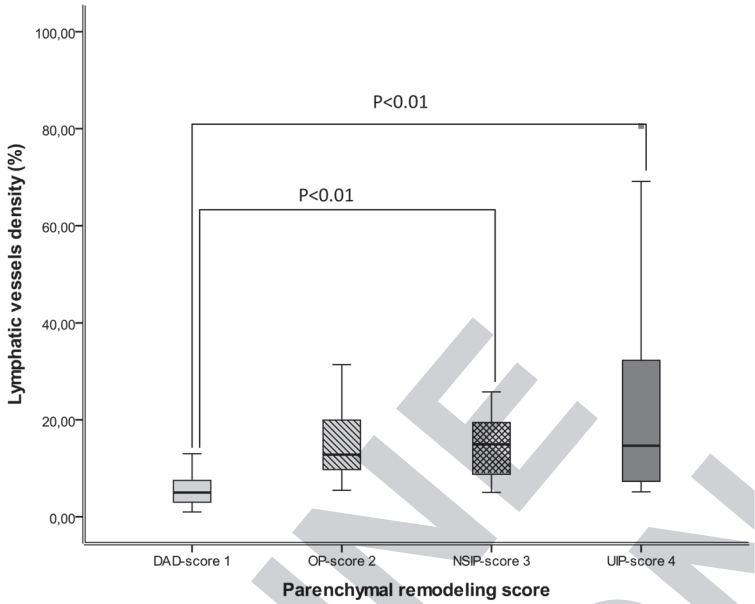

Figure 2. Lymphatic density according to score for the four lesions. Lymphatic D2-40+ in 10 fields of view observed by light microscopy at 400X magnification. The values of lymphatic D2-40+ are 6.66 ± 1.11 in diffuse alveolar damage (DAD), 15.35 ± 3.75 in organizing pneumonia (OP), 15.49 ± 1.80 in nonspecific interstitial pneumonia (NSIP), and 23.45 ± 5.24 in usual interstitial pneumonia (UIP). Lymphatic density increases from DAD score 1, OP score 2, NSIP score 3, up to UIP score 4 with a statistically significant difference. *P < 0.01 (ANOVA).

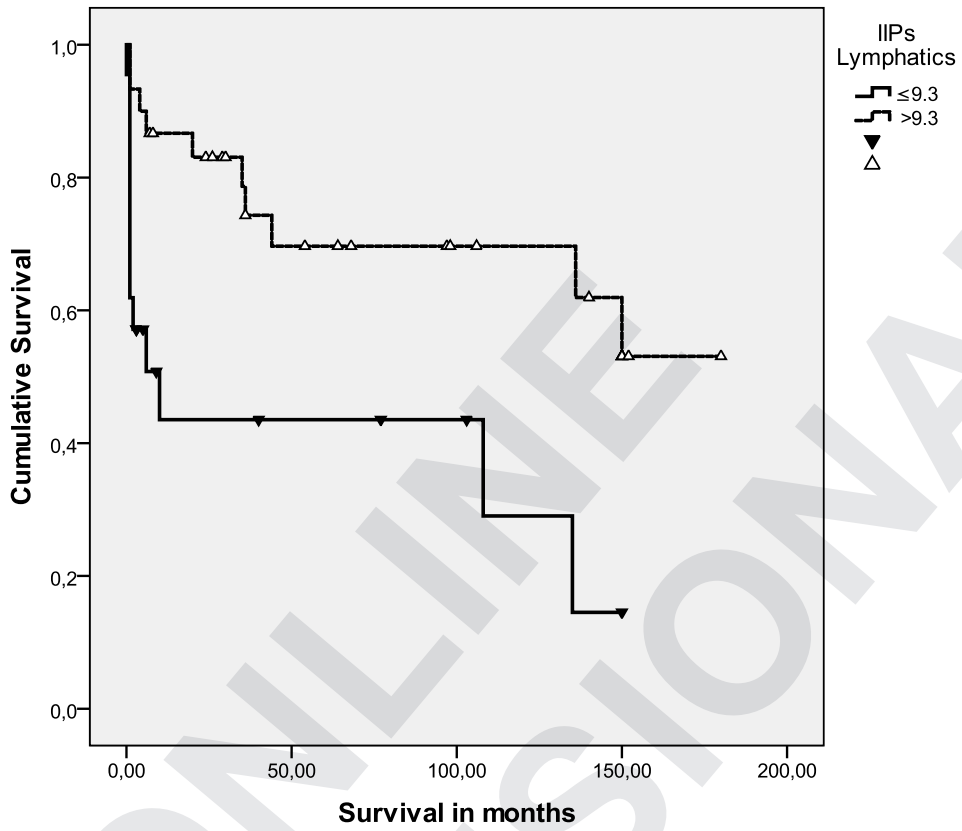

Figure 3. Multivariate analysis by Cox regression plots of survival probability versus follow-up time in months in patients with idiopathic interstitial pneumonia (IIP). The group with lymphatic density higher than 9.3% appears as the top curve, and the group with lymphatic density lower than 9.3% appears as the bottom curve (log likelihood = 61.98; P < 0.001).